RL-TR-96-81
Final Technical Report
May 1996

DEVELOPMENT OF A 100-GHZ ELECTRO-OPTIC MODULATOR

University of Michigan

John A. Nees and Steven L. Williamson

APPROVED FOR PUBLIC RELEASE; DISTRIBUTION UNLIMITED.

Rome Laboratory
Air Force Materiel Command
Rome, New York

This report has been reviewed by the Rome Laboratory Public Affairs Office (PA) and is releasable to the National Technical Information Service (NTIS). At NTIS it will be releasable to the general public, including foreign nations.

RL-TR-96-81 has been reviewed and is approved for publication.

APPROVED: Richard Payne

DR. RICHARD PAYNE
Project Engineer

FOR THE COMMANDER: Robert V. McGahan

DR. ROBERT V. McGAHAN
Director
Electromagnetics & Reliability Directorate

If your address has changed or if you wish to be removed from the Rome Laboratory mailing list, or if the addressee is no longer employed by your organization, please notify RL (ERO) Hanscom AFB MA 01731. This will assist us in maintaining a current mailing list.

Do not return copies of this report unless contractual obligations or notices on a specific document require that it be returned.

REPORT DOCUMENTATION PAGE

Form Approved
OMB No. 0704-0188

1. AGENCY USE ONLY (Leave Blank)	2. REPORT DATE	3. REPORT TYPE AND DATES COVERED
	May 1996	Final Apr 90 - Apr 93

4. TITLE AND SUBTITLE

DEVELOPMENT OF A 100-GHZ ELECTRO-OPTIC MODULATOR

5. FUNDING NUMBERS

C - F19628-90-K-0015
PE - 61102F
PR - 2305
TA - D7
WU - 12

6. AUTHOR(S)

John A. Nees and Steven L. Williamson

7. PERFORMING ORGANIZATION NAME(S) AND ADDRESS(ES)

University of Michigan
Ultrafast Science Laboratory
Ann Arbor MI 48109-2099

8. PERFORMING ORGANIZATION REPORT NUMBER

N/A

9. SPONSORING/MONITORING AGENCY NAME(S) AND ADDRESS(ES)

Rome Laboratory/ERO
80 Scott Drive
Hanscom AFB MA 01731-2909

10. SPONSORING/MONITORING AGENCY REPORT NUMBER

RL-TR-96-81

11. SUPPLEMENTARY NOTES

Rome Laboratory Project Engineer: Dr. Richard Payne/ERO/(617) 377-5128

12a. DISTRIBUTION/AVAILABILITY STATEMENT

Approved for public release; distribution unlimited.

12b. DISTRIBUTION CODE

13. ABSTRACT (Maximum 200 words)

This contract was designated for the development of technologies necessary to demonstrate hundred-gigahertz modulation of optical signals. Techniques are presented for eliminating velocity mismatch and model dispersion, which are the primary limitations on state-of-the-art modulators. Problems of interconnects and test instrumentation are treated and some additional work with related materials is discussed.

14. SUBJECT TERMS

Electro-optica modulator, High-voltage switching, Picosecond nanoprobe, Semiconductor optical temporal analyzer (SOTA)

15. NUMBER OF PAGES

32

16. PRICE CODE

17. SECURITY CLASSIFICATION OF REPORT	18. SECURITY CLASSIFICATION OF THIS PAGE	19. SECURITY CLASSIFICATION OF ABSTRACT	20. LIMITATION OF ABSTRACT
UNCLASSIFIED	UNCLASSIFIED	UNCLASSIFIED	UL

TABLE OF CONTENTS

INTRODUCTION: OBJECTIVES

Optical communication holds the potential for extremely high transmission rates. State-of-the-art system bandwidth, however, lags behind by two orders of magnitude the transmission bandwidth of optical fibers. One factor limiting the development of these higher-bit-rate systems is our inability to measure picosecond electrical transients present in optoelectronic components. Electro-optic sampling enables time resolution of electrical transients with subpicosecond precision.[1] With this capability, the development of modulators and detectors designed for bandwidths up to hundreds of gigahertz has become manageable.

This contract was designated for the development of technologies necessary to demonstrate hundred-gigahertz modulation of optical signals. We present techniques for eliminating velocity mismatch and modal dispersion, the primary limitations on state-of-the-art modulators. Problems of interconnects and test instrumentation are treated and some additional work with related materials is covered. In the sections that follow we describe the development of a wavelength-compatible modulator, and detector for operation in the multi-hundred-gigahertz regime, as well as high-power picosecond switching and the newly developed Semiconductor Optical Temporal Analyzer (SOTA) and picosecond nanoprobe.

Modulator

While optical fibers have potential for tremendous information capacity, current systems do not utilize a major portion of the available bandwidth. Modulators designed for low-voltage applications are currently limited to ~40 GHz.[2] In principle, a traveling-wave electro-optic modulator can be fabricated from GaAs, for modulation well above 100 GHz. To approach such performance requires the elimination of not only velocity mismatch, which limits state-of-the-art devices, but also dispersion of the microwave signal, radiation loss, and losses due to skin effect and free carrier absorption (Fig. 1).

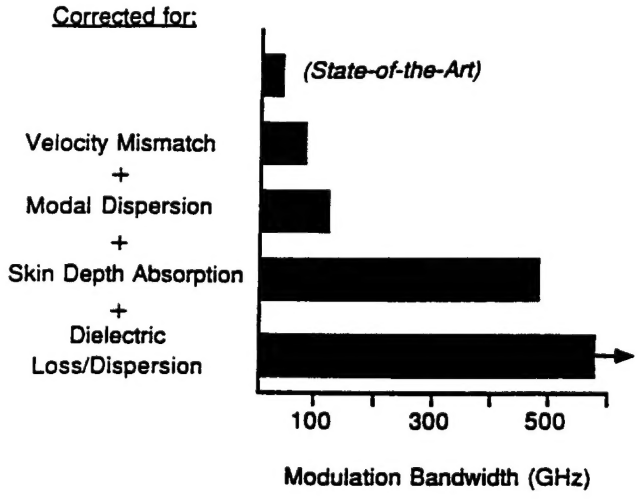

Figure 1. Fundamental limits for traveling-wave modulators

A primary source of dispersion, that is, velocity mismatch, may be eliminated by encapsulating the transmission lines in a uniform gallium arsenide (GaAs) medium. GaAs possesses the unique property of having bulk dielectric constants in the near infrared and millimeter-wave regimes that are essentially equal.[3] We have demonstrated that encapsulating a

transmission line in a uniform dielectric also eliminates frequency-dependent dispersion and radiation losses otherwise present due to dielectric mismatch. Beyond this, losses associated with skin effect, and free-carrier absorption have been mitigated by lowering temperature.

We have shown significant enhancement in bandwidth by applying an index-matched superstrate using an optically guided traveling-wave modulator.[4] In Fig. 2 a cross-sectional diagram of a GaAs traveling-wave modulator is shown, with a GaAs cover positioned over the transmission line electrodes. The modulator length is 4 mm. To test the bandwidth of the modulator a picosecond-rise-time electrical pulse is formed using photoconductive switching.[5] A 1-ps optical probe pulse at 1064 nm is synchronized to the electrical pulse using an adjustable delay and is focused into the optical waveguide. Figure 3 shows the correlation of the electrical and optical signals over the 4 mm interaction length as the optical pulse is delayed relative to the electrical pulse timing. The 3.2-ps rise time corresponds to a bandwidth of 110 GHz.

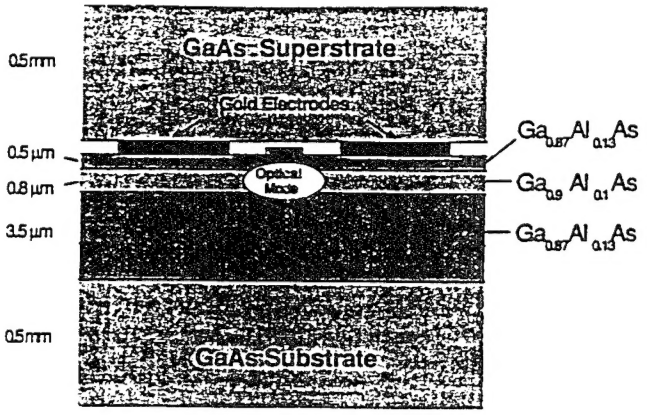

Figure 2. Cross-section of a 110-GHz traveling-wave modulator

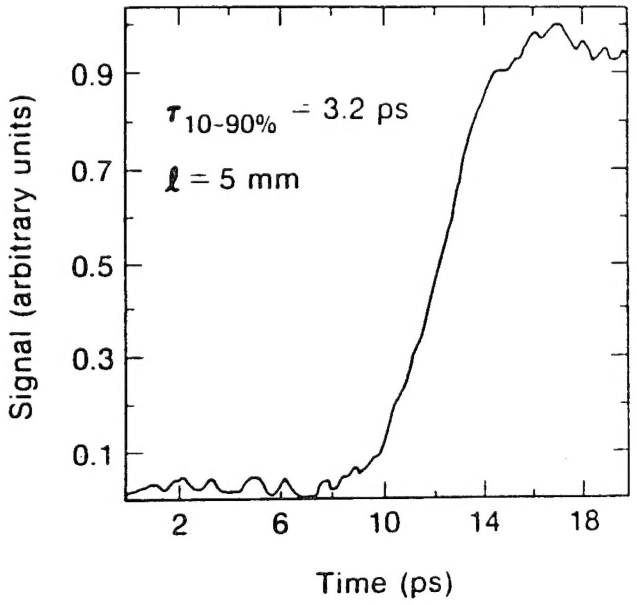

Figure 3. Correlation of a 1-ps optical pulse with a 1-ps electrical pulse on the modulator

This is the fastest traveling-wave modulator with 4-mm length demonstrated to date. However, many problems beset this initial device. The optical waveguide is lossy for the 1064 nm, resulting in a 20-dB optical insertion loss. Also, the half-wave voltage is 288 volts, four times greater than the calculated value. These two effects are coupled and are a consequence of carrier generation from the optical probe pulse. Operation at cryogenic temperatures acts to steepen the absorption edge for the AlGaAs, thereby lowering the attenuation factor and enhancing the electric field. Operation at 1300 nm or longer wavelength also markedly decreases free carrier absorption due to the fact that fewer mid-gap levels are excited.

To specifically test the propagation of electrical signals on the modulator we have constructed a coplanar transmission line fully encapsulated in unintentionally doped [001] GaAs. We first use a reactive-ion etch to form 280-nm-deep coplanar troughs into which 280 nm of gold is deposited. Electrodes 20 μm wide and separated by 20 μm are formed, leaving the top surface of the modulator flush. A scanning electron microscope (SEM) view of this structure is shown in Fig. 4. The dc linear resistance is 4.9 Ω/mm at 293 K and 0.8 Ω/mm at a temperature of 10 K.

A second crystal of GaAs is then placed on the modulator fully enclosing the coplanar electrodes with, at most, 20 nm of air interface. The two crystals are held in contact using spring-loaded clips to assure good contact. The presence of any air-gap at the interface alters the effective dielectric constant for the electrical signal. An air-gap of only 200 nm is sufficient to alter the propagation time by 2 ps over a 10-mm path.

External electro-optic sampling was used to characterize the electrical wave propagation in this device. A picosecond electrical transient propagated round-trip on the transmission lines, accumulating 10 mm of travel, before being measured (see Fig. 5). Figures 6 and 7 show the signals measured at 293 K and 10 K respectively. The input rise time at both temperatures is 1.3 ps. The output at 293 K is found to have been strongly attenuated and the rise time broadened to 3.0 ps for a response of 2.1 ps after deconvolving the input. Both attenuation and broadening are primarily due to skin effect attenuation by the gold electrodes. At 10 K the amplitude of the propagated signal is comparable to the input and the rise time is 2.0 ps, corresponding to a response of 1.4 ps and a bandwidth of 250 GHz. This broadening takes place over a total delay of 120 ps.

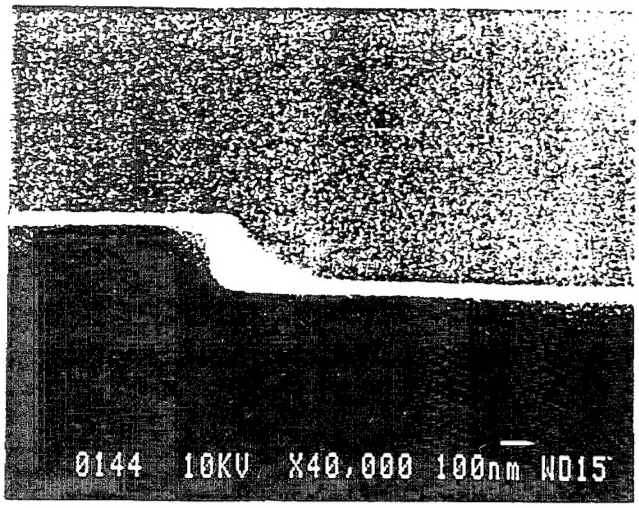

Figure 4 (a). Scanning electron view of 280-nm channels

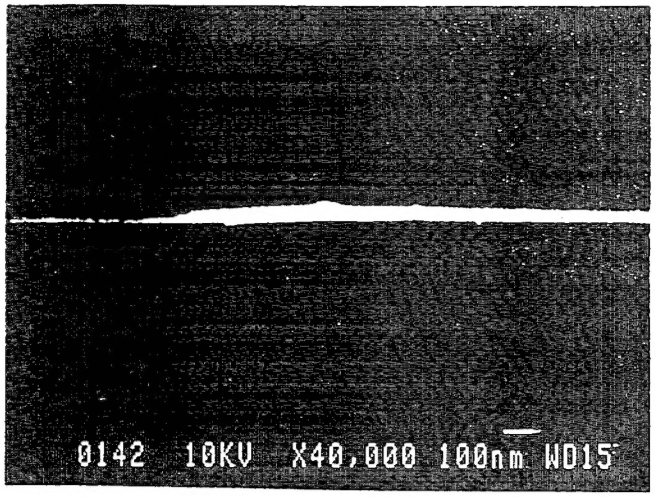

Figure 4 (b). Scanning electron view of flush coplanar striplines

Careful determination of the propagation time was made by measuring the optical path difference between optical pulses synchronized with the arrival of the input and output signals. With the propagation time and the length of the superstrate known, an accurate measurement of the effective dielectric constant can be determined. The effective dielectric constant for the covered transmission line structure was found to be 11.60 (+/- 0.02). This agrees remarkably well with the bulk value of GaAs at 1.3 μm, 11.62 [3]. The difference in arrival times between electrical and optical pulses propagating in this structure would be ~500 fs for a 10-mm interaction length. These results are qualitatively revealing. The use of a mechanically-applied GaAs superstrate serves to demonstrate the feasibility of velocity matching for hundred-gigahertz traveling-wave optoelectronic modulators. Practical use of this technique is being studied by regrowing GaAs over the substrate to form a superstrate that is an integral part of the device. Regrowth techniques are now being investigated for compatibility with high-bandwidth electrode structures.

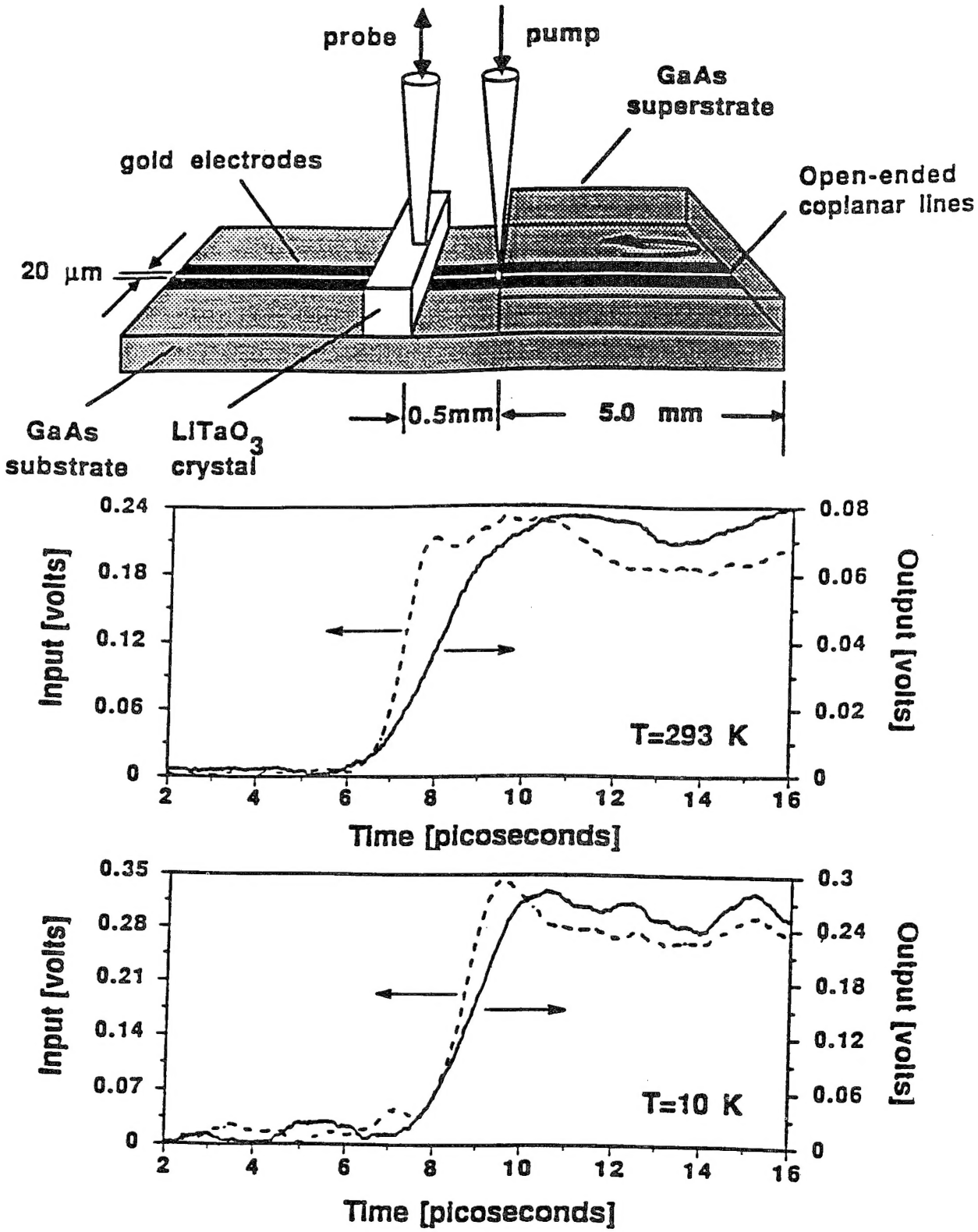

Figures 5, 6, & 7: 5. Illustration of the experimental measurement of electrical propagation delay
6. Input and output after 10-mm propagation at room temperature
7. Input and output after 10-mm propagation at 10 K

Detector

Also of key importance in the development of hundred-gigahertz optical communications is the detector. Much progress has been made over the past several years in the development of high-speed photodiodes. Detection bandwidths of 105 GHz with responsivities of 0.1 A/W have been reported for a metal-semiconductor-metal (MSM) photodiodes.[6] The most common approach to increasing the bandwidth in MSM photodiodes (at least up to 100 GHz) is the reduction of carrier transit time by reducing the electrode spacing. Achievement of bandwidths greater than 100 GHz, however, requires more than simply reducing further the electrode spacing. Simulation of the intrinsic response for a photodiode with 0.1-μm electrode spacing by Monte Carlo calculation shows a response tail persisting for picoseconds and having an integrated energy comparable to the main signal.[7,8] This tail is caused by the long transit time of the photogenerated holes, which can be almost 10 times that of electrons. This can be seen experimentally in Fig. 8, which shows the response of an interdigital MSM photodiode with 0.6-μm spacing on semi-insulating GaAs. As illustrated in Fig. 9, the persistence of conductivity is attributed to the low mobility of the holes which gives rise to low charge collection and recombination rates.

Response times of photoconductive detectors, on the other hand, can be quite fast because they are determined solely by the carrier lifetime of the material that is used. Low-temperature-grown GaAs (LT GaAs) has recently been used to perform ultrafast [9] and high-power [10] optical switching. The subpicosecond carrier lifetime,[11] high mobility (> 200 $cm^2/V \cdot s$), and high breakdown field strength (>100 kV/cm) of LT GaAs make it an ideal material for electrical pulse generation and gating. Such applications have thus far required the use of moderate-to-high peak optical powers since the switching efficiency (the ratio of electrical output power to optical input power) is still less than 1%. However, as we have found, the switching *efficiency* is influenced more by electrode dimensions than by intrinsic characteristics of the semiconductor material.

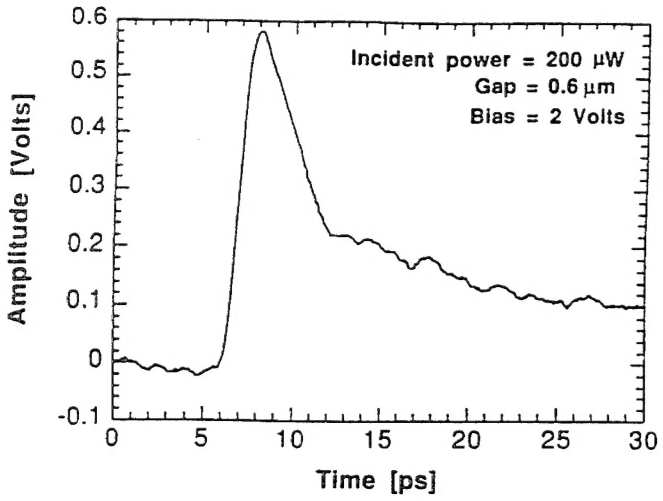

Figure 8. Response of a 0.6-μm interdigital MSM on GaAs

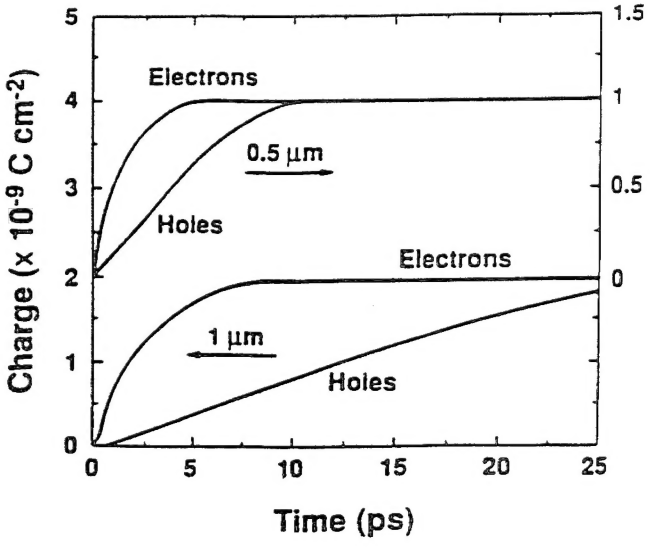

Figure 9. Electron and hole collection rates for 0.5- and 1-μm interdigital MSMs

We found that a LT-GaAs-based photoconductive detector that takes advantage of the high breakdown field capability of LT GaAs can have greatly improved sensitivity. In a photodiode, a reduction in electrode spacing tends to improve *speed* with little change in sensitivity. In a photoconductive detector, by contrast, such a reduction tends to increase the *sensitivity* with little change

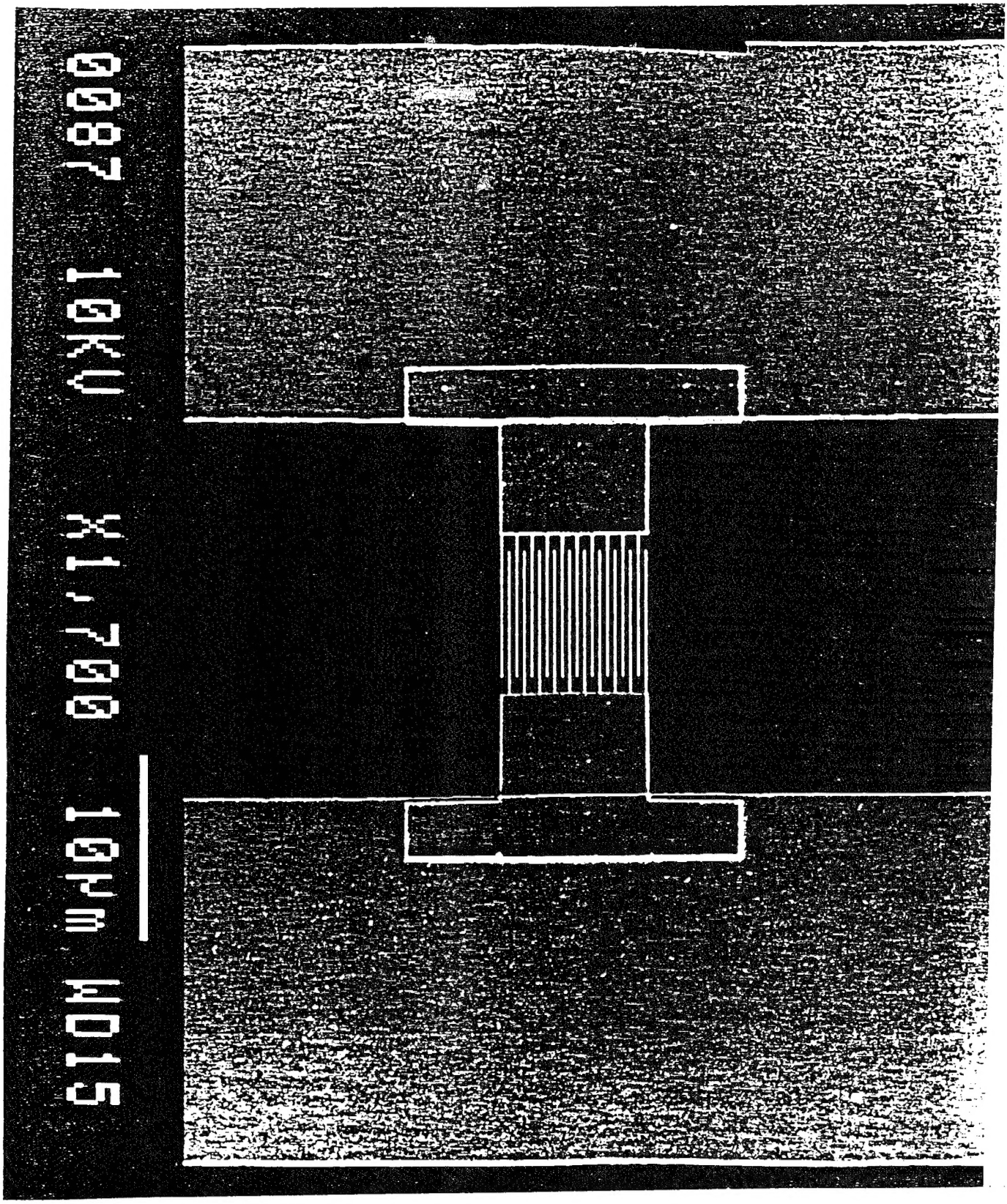

Figure 10. Scanning electron view of a 0.2-µm interdigital MSM on LT GaAs

in speed. Decreasing the carrier transit time across the semiconductor gap to a value approximate to the carrier lifetime results in an increase in the photocurrent gain to a value near unity.[12] For a carrier lifetime of 1 ps, this condition is met when the electrode spacing (the actual gap between electrodes) is about 0.1 μm. A further decrease in the electrode spacing could increase the photoconductive gain to still higher values, provided the metal-semiconductor contacts are ohmic. With unity gain, the responsivity of a LT-GaAs photoconductive detector is comparable to that of a photodiode, while its speed is still determined primarily by the (sub)picosecond intrinsic carrier lifetime.

Demonstrating this principle, we fabricated a LT-GaAs photoconductive detector with interdigital electrodes having finger widths and spacings of 0.2 μm, as shown in Fig. 10. A 1.5-μm-thick LT-GaAs layer was grown on a [100] semi-insulating GaAs substrate with a 0.4-μm-thick conventionally grown undoped buffer layer. The LT-GaAs layer growth was performed using molecular beam epitaxy at a substrate temperature of 190 °C, followed by annealing at 600 °C for 10 min in an arsenic overpressure. The interdigital electrodes were fabricated of 300-Å/2000-Å Ti/Au using direct-write electron-beam lithography in a JEOL JBX 5DIIF system. The detector's active area was 6.5 x 7.6 μm^2. Coplanar transmission line electrodes of 500-Å/2500-Å Ti/Au, with 20-μm widths and spacings and lengths of 5 mm, were also fabricated on the LT GaAs using optical lithography. For comparative purposes, similar structures were also fabricated with 0.6- and 1.0-μm finger spacings and widths in the same process. Referring to Fig. 10, the LT-GaAs photoconductive detectors were placed in coplanar transmission lines (Z_0 = 90 Ω) to assure good coupling of the generated electrical pulse to the propagating mode and also to eliminate parasitic losses. The detector was not antireflection-coated in this work. Reference transmission lines of identical dimensions, but without the interdigital detectors, were also fabricated on the wafer to determine overall system response. The technique of "sliding-contact" switching, which provides electrical excitation between the lines without the interdigital detector, can have a response less than 0.5 ps.[5] The photoconductive detectors were characterized using external electro-optic (EO) sampling [1]. A colliding-pulse, mode-locked dye laser operating at 610 nm with a repetition rate of 100 MHz was used to produce 150-fs pump and probe pulses. Electrical signals were measured on the transmission lines at a distance of 450 μm from the detectors. Although not shown in the figure, the EO sampling crystal spanned both the detector/transmission-line assemblies and the reference transmission lines, so that the translation of the pump and probe beams required to make either measurement was only ~ 200 μm.

A bias of 10 V dc could be applied to the detector before breakdown occurred, corresponding to a breakdown field strength of 500 kV/cm. This value is more than twice the highest that has been reported for LT GaAs under dc-bias conditions, which was obtained using 20-μm-spaced electrodes.[9] This result more accurately represents the actual breakdown field strength for LT GaAs, since our 0.2-μm electrode spacing confines the electric field to the 1.5-μm-thick LT-GaAs epilayer. A dark current of 100 pA was measured with 1 V applied to the detector. At 8 V (400 kV/cm), our measurement bias, the dark current increased to 300 nA. For an average optical power of 4 μW, the responsivity was measured to be 0.1 A/W. Past work using 20-μm-spaced electrodes on LT GaAs attained a responsivity of only 10^{-3} A/W.[13] The 100-fold reduction in gap dimension therefore corresponds to a 100-fold improvement in the responsivity. The value of 0.1 A/W is comparable to responsivities of high-speed photodiodes. Surface reflective losses from the interdigitated electrodes and the semiconductor amounted to 70% of the incident signal, so an internal quantum efficiency of 68% is calculated. The intrinsic carrier lifetime for the LT-GaAs sample was measured previously using time-resolved reflectivity[14] and found to be 0.6 ps. We calculate the capacitance [15] of our structure to be 4 fF, for an RC-limited response time of 360 fs in the 90-ohm transmission line structure. Figure 11 shows the response measured for the detector/transmission-line assembly and the sliding-contact switch on the reference

transmission line. Both measurements were made 450 μm from the point of signal generation. The optical pulse energy on the detector was 0.04 pJ, corresponding to an average power of 4 μW.

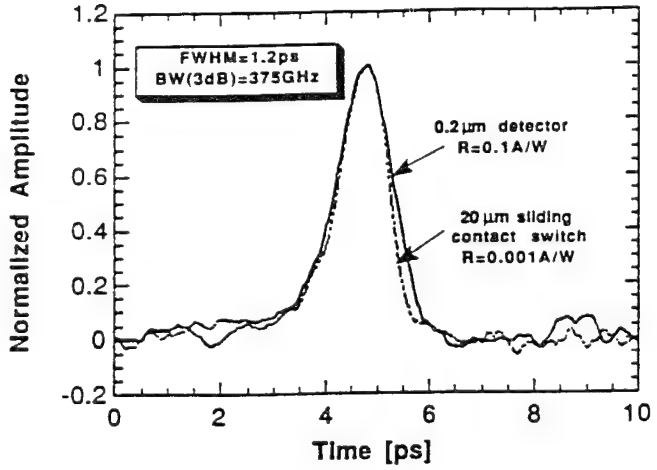

Figure 11. Temporal response of the photoconductive detector and sliding-contact switch measured 450 μm from the point of signal generation

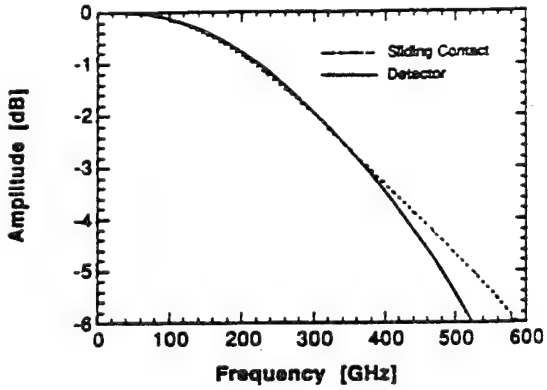

Figure 12. The -3-dB point for both signals occurs at 375 GHz

The detector response is 1.2 ps, full-width-at-half-maximum, with no evidence of a tail. To the contrary, the trailing edge, with a 10–90% fall time of 0.8 ps, is faster than the leading edge. We obtain a similar shape for the response of a sliding-contact switch on the reference transmission line. The fast tail is indicative of modal dispersion from quasi-TEM propagation along a transmission line having a substrate and superstrate with different dielectric constants.[16]

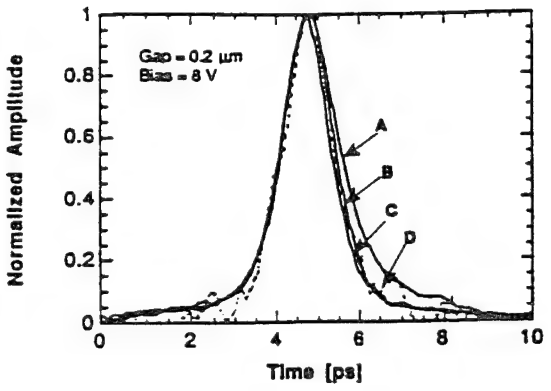

Figure 13. Set of four signals generated from the photoconductive detector, using 22 (A), 8.3 (B), 0.83 (C), and 0.04 (D) pJ, respectively

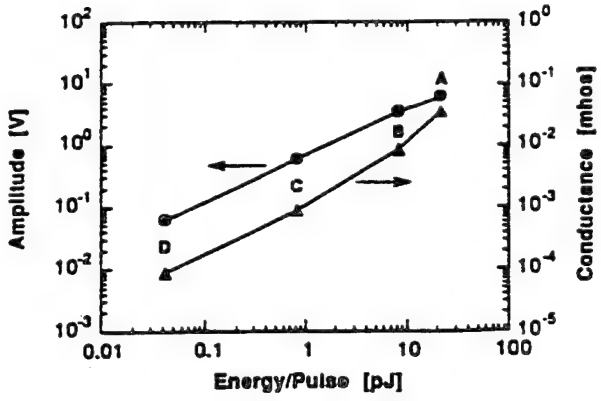

Figure 14. Peak amplitude vs. pulse energy for a 0.2-μm interdigital MSM on LT GaAs

Since these results are a convolution of the LT-GaAs intrinsic response time and such system-related factors as the RC time constant, laser pulse width, and electro-optic material response, the intrinsic response time for the interdigital detector may be subpicosecond. Figure 12 shows the -3–dB point for both signals occurring at 375 GHz. These curves were obtained by taking the discrete Fourier transform of the time-domain data. Waveforms for several values of pulse energy are shown in Fig. 13. The four signals, generated using 0.04-, 0.83-, 8.3-, and 22-pJ pulses, have peak amplitudes of 0.06, 0.6, 3.5, and 6 V, respectively. In Fig. 14 the peak amplitude and conductivity of these signals are plotted against optical pulse energy. We see that a nearly 500-fold increase in intensity extends the response only slightly from 1.2 to 1.5 ps. Under similar experimental conditions, a high-speed photodiode would suffer significant temporal broadening from low-frequency gain by photoinduced band bending[18] and from space charge.[17] Thus, the LT-GaAs photoconductive detector avoids the usual restriction of high-speed photodiodes to pulse energies below 0.1 pJ.

In Fig. 15 we show the electric-field dependence of the 0.2-μm detector response. These measurements were made with electric field strengths of 25 V/μm, 15 V/μm, and 5 V/μm. There is little change in the pulse width or decay time with electric field. A similar measurement, carried out with a 1.0-μm detector, is shown in Fig. 16. Here, there is a clear increase in decay time with an electric field as low as 10 V/μm. A possible explanation for the gap dependence on decay time involves the process of impact ionization.[19] When the electric field exceeds a certain value, photoinduced carriers can accelerate to sufficient energy levels to ionize additional carriers. The occurrence of impact ionization will increase the decay time as new carriers are freed in the process. The rate of ionization is dependent both on the electric field and on electrode spacing. The field in either structure is well above the threshold value for impact ionization. However, with much shorter electrode spacing, the process cannot fully develop.

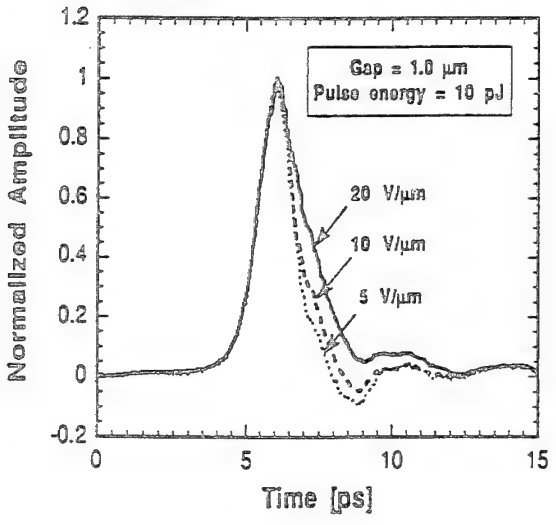

Figure 15. LT-GaAs photoconductive response as a function of electric field with electrode width and spacing of 0.2 μm,

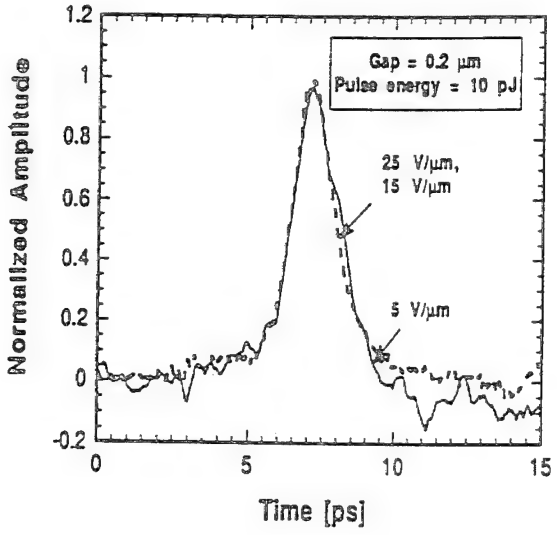

Figure 16. ... and with electrode width and spacing of 1.0 μm

In summary, we have developed a new MSM-type photoconductive detector, based on LT GaAs, using 0.2-μm-spaced interdigital electrodes. The response time measured by EO sampling is 1.2 ps. Without an antireflective coating the detector has a responsivity of 0.1 A/W. To our

knowledge, this is the fastest high-sensitivity detector of any kind reported to date. In addition, it can be driven to an on-state resistance as low as 30 Ω with little degradation in speed. This versatility permits the device to function both as a detector and a gate. In the gate mode, the device can perform either as a high-contrast sampler with a picosecond window or as an efficient picosecond electrical-pulse generator. This unique dual functionality together with ease of integration will permit a number of detector elements to be combined for acquisition and processing single-picosecond optical and electrical events with high efficiency and minimal temporal distortion.

High-Power Switching

The unique properties of the LT-GaAs material which make it attractive for high-speed MSM photoconductors also give it a distinct advantage in other applications which push the limits of speed, field breakdown potential and dark resistivity. To further explore the utility of these epilayers we have conducted a study of photoconductive switching at the kilovolt level with peak currents approaching 20 amps.

Recently many applications have emerged for high-voltage, high-speed switching. The only technique now available for achieving kilovolt electrical pulses with picosecond rise times is laser-driven photoconductive switching. Generation of a 1-kV pulse with a rise time of 12 ps and a pulse width of 70 ps has been reported.[20] This was done using a high-resistivity semiconductor with a 1.5-mm switch gap. The fastest rise time possible for this switching structure can be determined by calculating signal propagation time over the electrode separation at the switching gap. For this size gap that time is ~12 ps. Using electrodes separated by 10 μm, subpicosecond duration electrical pulses with amplitudes up to 6 volts have also been generated.[13] The constraints of having a large photoconductive gap to hold off high voltage and a small gap to maintain high speed have hitherto prevented kilovolt-amplitude, single-picosecond pulse generation.

With LT GaAs it is possible to fabricate extremely high-resistivity, high-breakdown threshold switches. Now, dc electric fields in excess of 10^5 V/cm are routinely achieved. It is also possible to pulse-bias the switching element for times shorter than breakdown,[1] avoiding thermal runaway and impact ionization. Using LT GaAs and pulse biasing we have applied up to 1.3 kV to a 100-μm gap. With this gap dimension, switching of the kilovolt-bias requires less than 1 μJ of optical energy, obtained from an amplified subpicosecond dye laser.

A schematic diagram of the experiment is shown in Fig. 17. The laser generates 2-μJ, 150-fs pulses at 620 nm with a 2-kHz repetition rate, using a two-stage dye amplifier pumped by a frequency-doubled Nd:YAG regenerative amplifier.[21, 22] Part of the frequency-doubled Nd:YAG regenerative amplifier output is used to photo-excite a dc-biased 4-mm-long semi-insulating GaAs switch which is used as the pulse-bias source. The switch is mounted in a microstrip line geometry between a ~10-Ω charge line and a 90-Ω coplanar transmission line. When illuminated by 80-μJ, 80-ps optical pulses at 532 nm, this device produces electrical pulses which have an amplitude equal to 70% of the dc-bias voltage (up to 2 kV) and a duration of 400 ps. The pulses then bias a 90-Ω coplanar stripline (100-μm wide gold conductors separated by 100 μm) on a LT-GaAs substrate. As the bias pulse propagates on the transmission lines, 150-fs, 100-nJ optical pulses excite a 100-micron-square area between the lines. The high density of carriers formed within the LT GaAs acts to short the electrodes. This form of sliding-contact switching, in principle, allows total switching of the applied bias voltage [5]. Electro-optic sampling [1] in a $LiTaO_3$ crystal with a 150-fs pulse is used to measure signal waveforms 300 μm from the switch site. In this system the crystal has a half-wave voltage of ~ 4 kV, insuring a response linear within 2% over the range of voltages measured. The +/- 5% calibration error of the

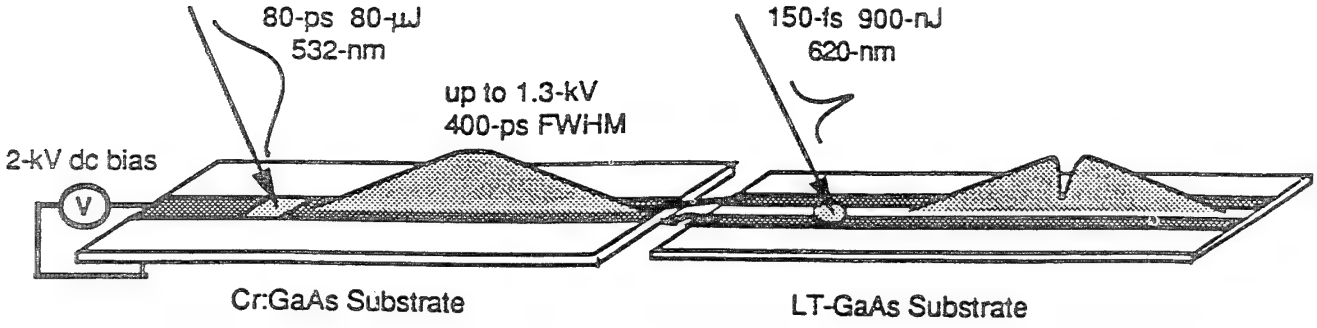

Figure 17. High-power-switching experimental setup

measurement is estimated to be caused mainly by laser intensity fluctuations. Waveforms are recorded for different settings of bias voltage and optical energy.

Figure 18 shows an 825-V pulse waveform with a rise time of 1.4 ps and a 4.0-ps duration (full-width-at-half-maximum). The negative precursor to the pulse is attributed to the radiation from the changing dipole formed at the generation site. For incident optical energies above 500 nJ we note saturation of the voltage-switching efficiency, defined as the ratio of switched voltage to applied voltage, as shown in Fig. 19. While the maximum efficiency is ideally 100%, the 70% experimentally measured can be explained by a combination of factors including dispersion and radiation of the propagating electrical pulse as well as by contact resistance on the LT GaAs.

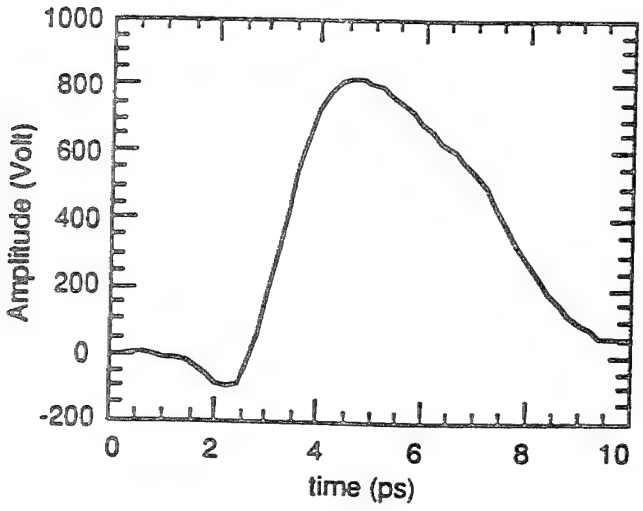

Figure 18. 825-V pulse switched on 100-μm co-planar transmission lines on LT GaAs

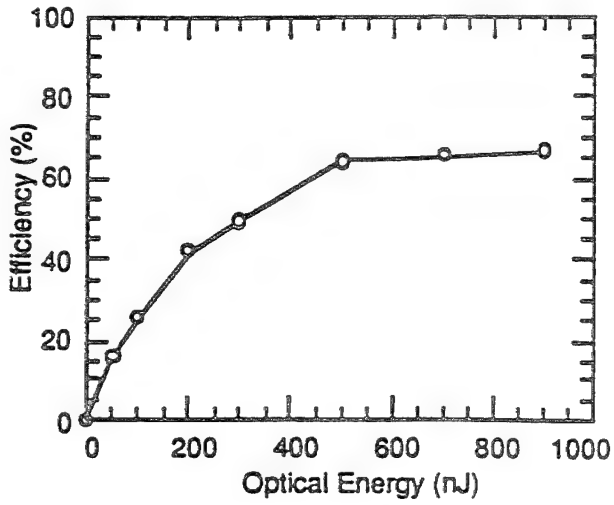

Figure 19. Switching efficiency (voltage switched/ voltage biased) vs. optical energy

The rise time is ultimately limited by the 100-μm transmission line dimensions, but we also find a clear dependence on the carrier density. As illustrated in Fig. 4, we see a degradation from 1.1 ps to 1.5 ps over the range of optical energy from 100 to 900 nJ. This is a saturation of the slew rate. The rise time nevertheless appears to be independent of the electric field (Fig. 5).

The relation of the slew rate to the carrier density is still not well understood. Explanations involving saturation of the current density and strong carrier scattering are presently being investigated.

Although a subpicosecond recombination time was anticipated from lower voltage work,[13] our measurements reveal a much longer recovery time. The recovery time was also found to increase when either the carrier density or applied electric field were increased (Figs. 20 and 21). Significant local heating due to the extremely high current densities (up to 10^7 A/cm^2) drawn through the switch area, resulting in the generation of additional carriers, could explain the long recovery time.

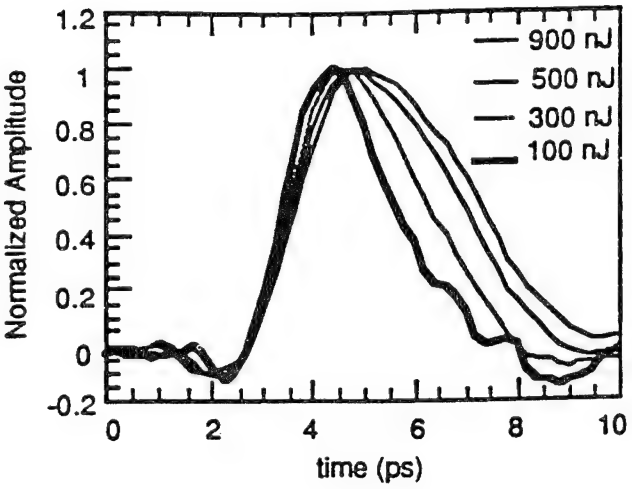

Figure 20. Switch response for different optical pulse energies

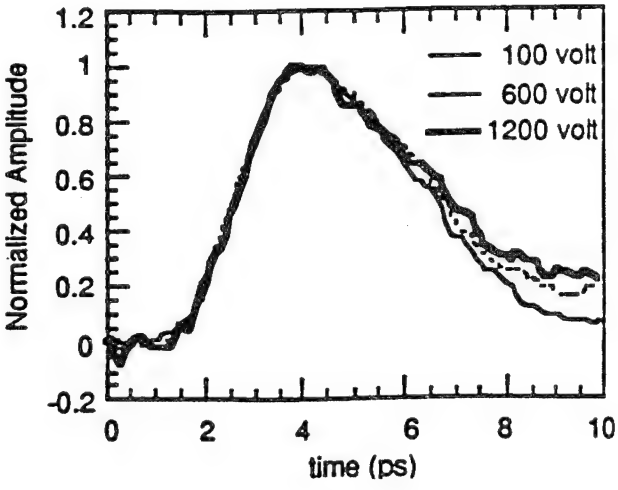

Figure 21. Switch response for different applied voltages

Another explanation for the long recombination time involves intervalley scattering, which is known to be strongly dependent on both electric field and carrier density. The pulse shape reflects the evolution of the current density, which is proportional to the product of carrier density and average carrier velocity. In GaAs, a photogenerated hot electron under the influence of a strong electric field can scatter from the central valley to the high-effective-mass satellite X- and L-valleys increasing its effective mass and its ability to produce current.

Scattering probability for carriers in the central valley increases with the electrical field and, under our experimental conditions, we estimate that more than 80% of the carriers scatter into the satellite valleys within 100 fs.[23] The reinjection of those electrons back into the central valley can take several picosecond.[24] As the pump energy increases, the carrier density in the central valley does also. Consequently, the probability for an electron to scatter back into the central valley is decreased. As the carriers in the central valley recombine (within a few hundred femtoseconds for LT GaAs), the probability of carrier transfer from the satellite valleys back to the central valley increases. The satellite valleys can then be seen as sources reinjecting hot electrons into the central valley at a rate dependent on the relative carrier populations, and is therefore a function of both optical fluence and electric field. This process causes current to persist until all carriers transfer back to the central valley where they either are trapped or recombine.

In conclusion, we report on the application of LT GaAs for photoconductive switching using a pulse bias and leading to the generation of a 825-V pulse with 1.4-ps rise time and duration

of 4.0 ps. This is the highest voltage ever obtained on the single-picosecond time scale. This new capability to produce ultrashort, high-peak-power electrical pulses should be of interest for applications in fields such as nonlinear millimeter-wave spectroscopy, radar, high-energy physics, and ultrafast instrumentation.

Semiconductor Optical Temporal Analyzer (SOTA)

Using far lower power levels high-speed, high-sensitivity photodetectors have been studied in other groups using picosecond photoconductive sampling.[25] Although the emphasis has been placed on the characterization of the detector,[26, 27] the combination of high-speed detector and sampling gate can also be viewed as a high-speed optical correlator. To our knowledge, this configuration has not yet been used to measure optical waveforms. This is due, in part, to the slow detectors that have been available. To have the highest speed and sensitivity requires more than simply a fast detector. Both the detector and gate must have high speed *combined* with high sensitivity.

In this section we describe a novel 1.2-ps photoconductive detector that functions with high performance in either detection or gating mode, permitting monolithic integration of the two elements. This is the key ingredient in the development of the SOTA.

Figure 22 illustrates the experimental setup for the SOTA. It is comprised of a fast photoconductive detector and photo-gate, integrated with a coplanar transmission line structure. The fast gate samples the electrical replica of the optical signal produced by the detector. The gate is spaced 100 μm from the detector. The gate electrode, extending perpendicular to the transmission line, is 1 mm in length. The detector and gate are identical to one another and to the detector previously described. A CPM dye laser is used as the pump and probe source. The gate beam has an average power of 3 mW, while the pump beam is adjustable from 8 nW to 3 mW. A pulse repetition rate of 100 MHz is used for these measurements. This leads to an average power-to-pulse energy conversion factor of 10^{-8} J/W.

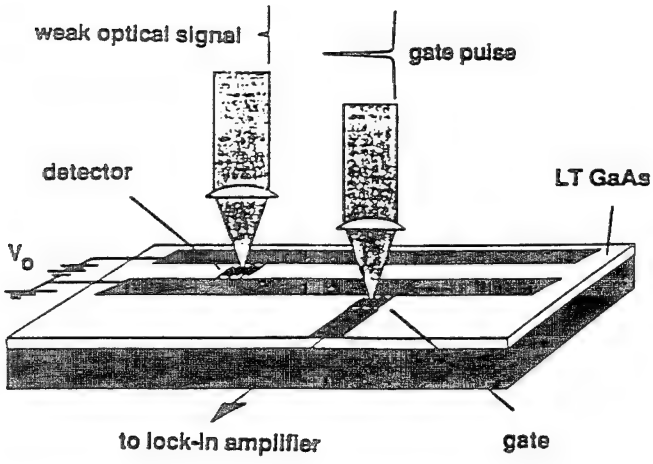

Figure 22. Experimental setup for testing the SOTA. The detector and gate are identical to one another and to the detector in Fig. 10.

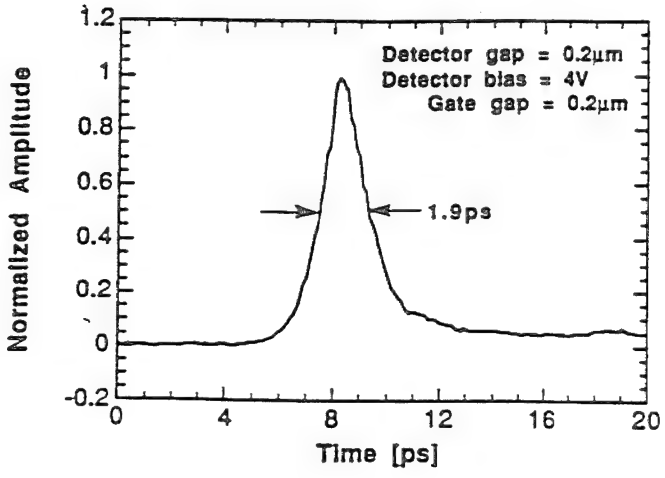

Figure 23. Temporal response from the SOTA

Thus, 3-mW average power corresponds to 30-pJ pulse energy. The pump beam is chopped at the lock-in frequency of 500 Hz. The output from the gate is amplified using a low-noise current amplifier set at 10^{-7} volts/amp. This signal is further amplified using a lock-in amplifier. Figure 23 shows a typical correlation curve measured with an average power on the detector of 1 MW (10 pJ/pulse). The system response is 1.9 ps, matching the convolution of the detector (1.2 ps) and the gate (1.5 ps) responses. We notice that the correlation trace maintains a trailing edge. This tail was found to be independent of either pump or gate pulse energy, indicating a possible rf-coupling effect to the gate electrode. The measured noise-equivalent-power (NEP), defined as the average optical power required to produce a signal-to-noise of one in a 1-Hz averaging bandwidth, is 500 pW, corresponding to a pulse energy of 5×10^{-18} J.

The theoretical NEP for the SOTA is ultimately determined by the thermal, or Johnson, noise at the gate.[28] Thermal noise current is given by

$$i_{thermal} = \sqrt{4kTG} \cdot \frac{A}{\sqrt{\text{Hz}}}$$

where k is the Boltzmann constant, T is the temperature, and G is the average conductance of the gate. The gate resistance is >10 MΩ in the off-state and 30 Ω in the on-state. With a duty cycle of 10^{-4} (1-ps gate window per 10 ns pulse period), this is equivalent to an average gate conductance of 3.4×10^{-6} mhos. At room temperature, the thermal noise current is 2.4×10^{-13} A/Hz$^{1/2}$. With a responsivity of 0.1 A/W this corresponds to a theoretical NEP of 2 pW. The large discrepancy between the theoretical and measured NEP values is due largely to large rf pickup noise from the surrounding environment.

It should be noted that this expression for thermal noise assumes that the carrier collision time is much faster than either the carrier lifetime or transit time.[29] With LT-GaAs, the carrier collision time is comparable to carrier lifetime. Therefore, a theoretical NEP of 2 pW may, in fact, be a conservative value.

We also see from this expression that thermal noise current increases as the square root of gate conductance. Signal current, on the other hand, increases linearly with gate conductance. The highest signal-to-noise is achieved when the gate is completely open. An upper limit for the gate conductance is imposed by the onset of carrier saturation. This effect, evident from the intensity-dependent temporal broadening seen in Fig. 5, already degrades system response by 10%.

In short, we take advantage of the features of the newly developed MSM photoconductive detector on LT GaAs to demonstrate a picosecond-resolution, semiconductor optical temporal analyzer (SOTA). The measured NEP for the device is 500 pW. The technique is jitter-free, permitting long integration times for ultraweak picosecond fluorescence and scattering experiments. Other ultrafast phenomena can be time resolved using this relatively simple tool.

Picosecond Nanoprobe

Continuing advances made in the development of semiconductor devices have pushed the speed of some devices to frequencies in excess of 400 GHz.[30] To test devices with this response requires the development of new probing techniques, capable not only of high temporal and spatial resolution, but also of noninvasive inspection. Purely electronic measurement instruments, such as vector network analyzers, spectrum analyzers, and sampling oscilloscopes, are not adequate tools for testing state-of-the-art high-speed integrated circuits. The rf network analyzers, which are now gaining acceptance for use up to 100 GHz, still have difficulties with test-fixture transitions, de-embedding of parasitic parameters, and overall accuracy and convenience of operation. Also, internal nodes cannot be tested at high speeds with the low-impedance probe technology that is now available for use with such instruments.

In contrast to all electronic techniques, electro-optic measurements have many unique features for high-speed circuit testing. The major attribute gained from this combination of optics and electronics is speed—both in temporal resolution and in acquisition time. External-probe electro-optic (EO) sampling has a temporal resolution as fast as 250 fs (>1 THz bandwidth) and offers the highest degree of flexibility of any optically based technique now available.[1] External EO sampling uses small (50-μm^2) tips of electric-field-sensitive material ($LiTaO_3$ or $LiNbO_3$) to make measurements of fringing electric fields that extend above the circuit under test. In developing applications for this probe technology, extending from high-speed, non-loading pin testing of packaged devices, to the development of a 100-GHz electro-optic network analyzer for testing of high-speed discrete analog devices,[31] we have also encountered limitations in spatial resolution (~5 μm) and signal sensitivity (>10 mV/√Hz). Also, absolute voltage measurements are subject to interpretation.

Utilizing LT GaAs we have recently developed a new optically based external probe that promises to overcome these limitations while maintaining a temporal resolution of 1 ps. The probe is based on photoconductive (PC) sampling, which has the highest sensitivity of any optically based sampling technique.[32] The probe we developed has a sensitivity of 4 $\mu V/\sqrt{Hz}$ and is capable of measuring the absolute voltage of the device under test.[33] With a dynamic range > 10^6 it is possible to measure from the microvolt to the 10-volt level. The probe, though contacting in nature, is relatively non-invasive with a load resistance of > 100 kΩ and a capacitance of < 10 fF.

It makes contact to the device under test using a conical tip which will have a tip radius of < 100 nm. As it operates as an absolute voltage probe, the sensitivity and speed of the measurements are independent of the tip-to-device contact resistance up to 10 kΩ.

To make submicron spatial resolution possible in testing integrated circuits, we have we have adapted the technology for forming metallic cones from the field of vacuum microelectronics.[34, 35] The process employs conventional, photolithographic techniques to form tips with a 100-nm radius of curvature (Fig. 24). This is done in the following way: on a substrate

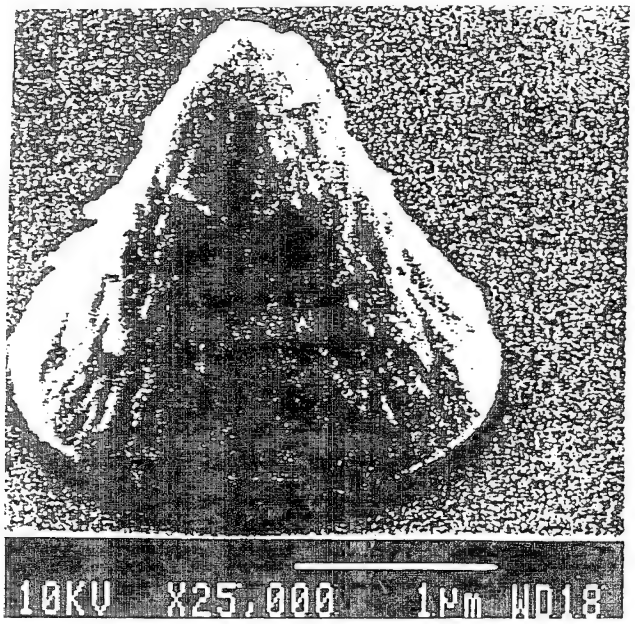

Figure 24. Scanning electron view of submicrometer tip formed by depositing titanium through a 3-mm self-closing hole

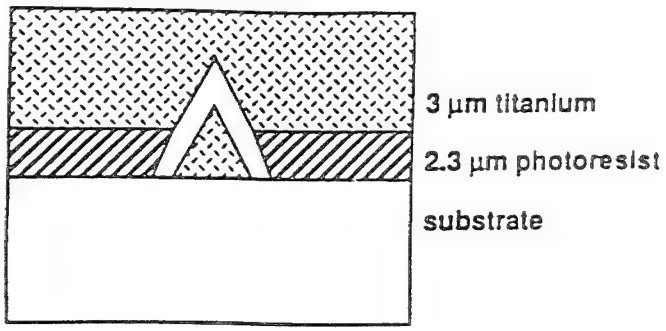

Figure 25. Process for forming the submicrometer tip

suitable for photolithographic processing, a thick layer of photo-resist is hardened, patterned, and developed, leaving a 3-μm round hole at the location where a tip is desired. Deposition of a few microns of metal, such as titanium or aluminum, simultaneously causes the growth of a conical tip at the base of this hole and the narrowing of its opening. This forms a sharp tip by virtue of the shrinking-aperture.

When the thick metallization is removed by dissolving the photo-resist layer, as shown in Fig. 25, a sharp, rugged tip remains fixed to the substrate. This recipe is compatible with a many other processes for GaAs and Si devices.

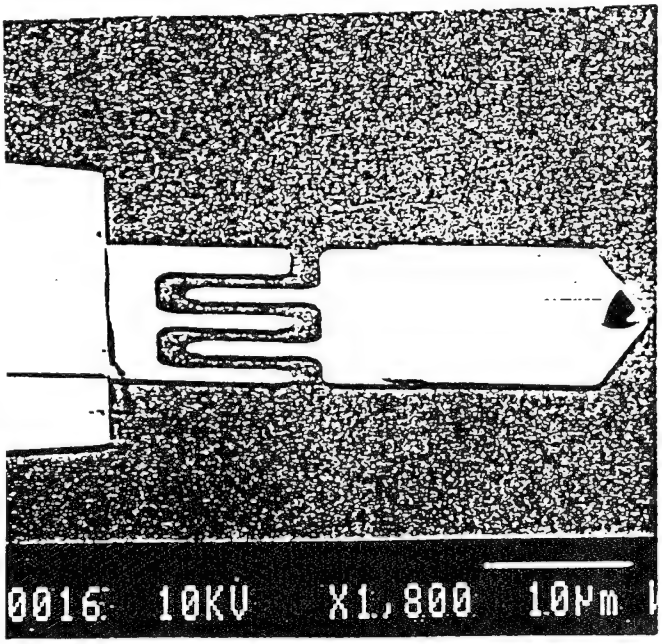

Figure 26. Scanning electron view of the integrated MSM gate and submicrometer tip on LT GaAs

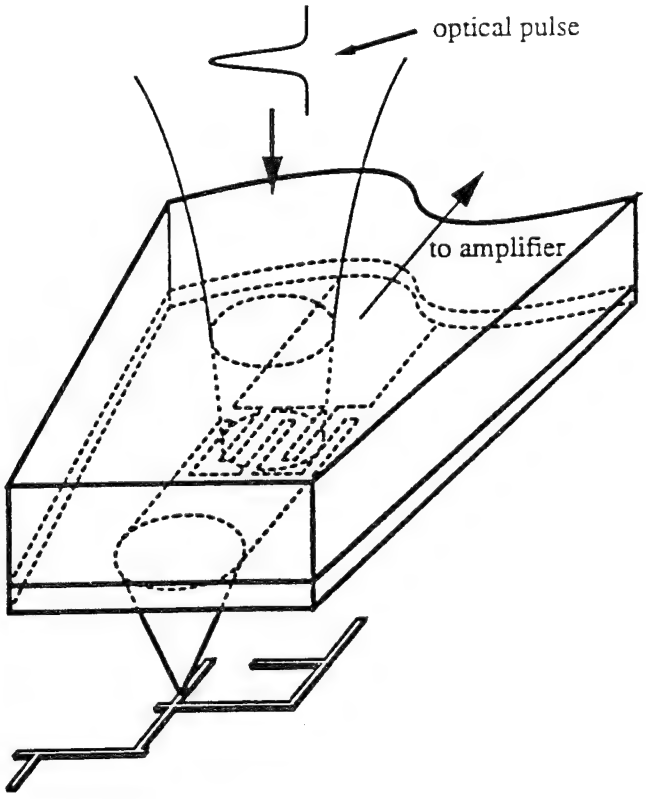

Figure 27. Position of nanoprobe relative to device under test

Figure 26 shows a photomicrograph of a photoconductive gate integrated with a submicron tip. Figure 27 illustrates a typical setup for using the photoconductive probe. To facilitate optical access to the gate, we can illuminate from the backside. This is accomplished by thinning the backside to a thickness of a few micrometers. For this approach, a 2-μm-thick layer of $Al_{.70}Ga_{.30}As$ is grown beneath the LT GaAs layer as an etch stop. Light then passes through the thin, transparent AlGaAs layer to excite the photoconductive gate. Alternatively, we use adhesive to fix the semiconductor to an independent substrate.

This high-speed, high-sensitivity probe was fabricated and tested in our laboratory. With a crude 20-μm square tip with a 2-μm interdigital photoconductive sampling gate on LT GaAs, the

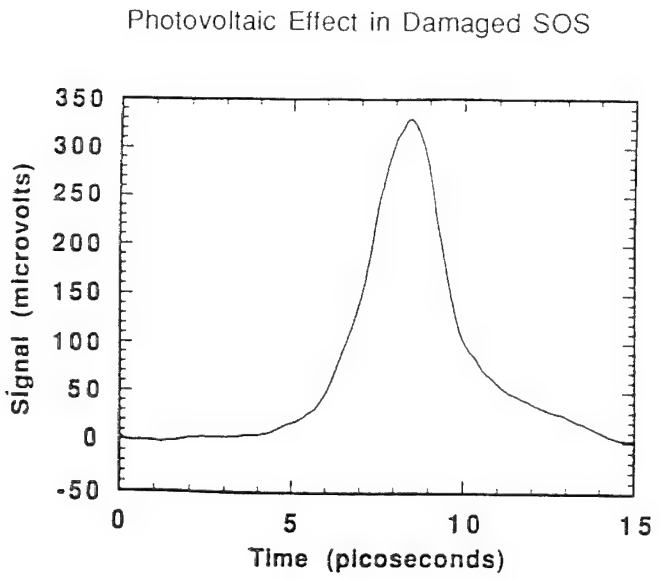

Figure 28. Measured waveform using a probe with a 20-μm tip

following results have been obtained: [34]

- Sensitivity of ~ 4 $\mu V/\sqrt{Hz}$ (the noise floor measured in Fig. 28);
- Temporal resolution of 2.3 ps;
- Measurement of absolute voltages was demonstrated;
- Repeatable contact was demonstrated;
- 30-ps gate delays in a heterostructure insulated-gate field-effect transistor (FET) enhancement/depletion mode inverter were measured;
- The probe was used in pulse mode to inject a picosecond signal onto transmission lines; and
- A second probe was used to time-resolve these picosecond response.

The variety of these results demonstrates the versatility of the photoconductive probe technology. The sensitivity of the external photoconductive sampling technique is also demonstrated by the low noise of the signal shown in Fig. 28.

SUMMARY

The work carried out under this contract has yielded steady progress en route to multi-hundred-gigahertz communications. The conditions for velocity matching and high-fidelity signal transmission in an optical modulator have been achieved. A high-speed photoconductive detector has been developed. New means of testing fast optical transients have been developed. A probe which has the potential to test devices and circuits in the hundred-gigahertz range has been demonstrated. These key points are outlined below:

Modulator

- Propagation speed of electrical signals matches optical signal speed to within two parts in a thousand. This corresponds to < 500-fs walk-off in 10 mm.
- 1.4-ps pulse response is preserved over 10 mm of propagation at reduced temperatures.
- 2.1-ps pulse response is maintained over 10 mm of propagation at room temperature.

Detector

- An MSM photoconductive detector based on LT GaAs is demonstrated to have a 375-GHz bandwidth (-3–dB point), 0.1 A/W responsivity, and utility in picosecond detection and gating.

High-Voltage Switching

- 825-Volt pulses are switched in LT GaAs with a 1.4-ps rise time and a 4-ps width in a 100-μm-wide transmission line gap.

SOTA

- An optical sampling structure based on the LT-GaAs MSM photoconductive detector/gate is shown to have 1.9-ps temporal resolution and pW sensitivity.

Picosecond Nanoprobe

- A new external circuit probe based on the MSM technology is demonstrated with 2.3-ps temporal resolution and absolute microvolt sensitivity.

REFERENCES

1. Whitaker, J. F., Valdmanis, J. A., Frankel, M. Y., Gupta, S., Chwalek, J. M., and Mourou, G. A., Microelectronics Engineering, Vol. 12, p. 369, 1990.
2. Korothy, S. K., Eisenstein, G., Tucker, R. S., Veselka, J. J., and Raybon, G., Applied Physics Letters, Vol. 50, p. 1631, 1987.
3. Palik, E. D., Handbook of Optical Constants and Solids, Academic Press Inc., 1985, p. 433.
4. Nees, J., Williamson, S., and Mourou, G., Applied Physics Letters, Vol. 54, p. 1962, 1989.
5. Grischkowsky, D. R., Ketchen, M. B., Chi, C.-C., Duling, I. N., Halas, N. J., and Halbout, J.-M., IEEE Journal of Quantum Electronics, Vol. 24, p. 221, 1988.
6. Van Zeghbroek, J., Patrick, W., Halbout, J.-M., and Vettiger, P., IEEE Electron Devices Letters, Vol. 9, p. 527, 1988.
7. Koscielniak, W. C., Pelouard, J. L., and Littlejohn, M. A., Applied Physics Letters, Vol. 54, 567 (1989).
8. Koscielniak, W. C., Pelouard, J. L., and Littlejohn, M. A., IEEE Photonics Technology Letters, Vol. 2, p. 125, 1990.
9. Smith, F. W., Le, H. Q., Diadiuk, V., Hollis, M. A., Calawa, A. R., Gupta, S., Frankel, M., Dykaar, D. R., Mourou, G. A., and Hsiang, T. Y., Applied Physics Letters, Vol. 54, p. 890, 1989.
10. Motet, T., Nees, J., Williamson, S., and Mourou, G., Applied Physics Letters, Vol. 59, p.1455, 1991.
11. Whitaker, J. F., Valdmanis, J. A., Frankel, M. Y., Gupta, S. J., Chwalek, M., and Mourou, G. A., Microelectronics Engineering, Vol. 12, p. 369, 1990.
12. Sze, S. M., Physics of Semiconductor Devices, 2nd ed., Wiley, New York, 1981, p. 746.
13. J. A., Frankel, Whitaker, J. F., Mourou, G. A., Smith, F. W., and Calawa, A. R., IEEE Transactions on Electron Devices, Vol. 37, p. 2493, 1990.
14. Gupta, S., Pamulatpati, J., Chwalek, J., Bhattacharya, P. K., and Mourou, G., in Ultrafast Phenomena VII, edited by C. B. Harris, E. P. Ippen, G. A. Mourou, and A. H. Zewail, Springer-Verlag, Berlin, 1990, p. 297.
15. Soole, J. B. D., and Schumacher, H., IEEE Transactions on Electron Devices, Vol. 37, p. 2285, 1990.
16. Gupta, S. J., Whitaker, J. F., and Mourou, G. A., IEEE Microwave Guided Wave Letters, Vol. 1, p. 161, 1991.
17. Moglestue, C., Rosenzweig, J., Kuhl, J., Klingenstein, M., Lambsdorff, M., Axmann, A., Schneider, J., and Hulsmann, A., Journal of Applied Physics, Vol. 70, 2435 (1991).
18. Rogers, D. L., Picosecond Electronics and Optoelectronics II, edited by F. J. Leonberger, C. H. Lee, F. Capasso, and H. Morkoç, Springer-Verlag, Berlin, 1987.
19. Sze, S. M., Physics of Semiconductor Devices, 2nd ed., Wiley, New York, 1981, p. 45.
20. Stearns, D. G., Journal of Applied Physics, Vol. 65, No. 3, p. 1308, 1989.

21. Norris, T., Sizer, T., and Mourou, G., "Generation of 85-fs Pulses by Synchronous Pumping of a Colliding Pulse Mode-locked Dye Laser." Journal of the Optical Society of America B, Vol. 2, April 1985.

22. Duling, I. N., Norris, T., Sizer, T., Bado, P., and Mourou, G., "Kilohertz Synchronous Amplification of 85-fs Optical Pulses." Journal of the Optical Society of America B, Vol. 2, April 1985.

23. Iafrate, G., "High-Speed Transport in III-V Compounds" in Gallium Arsenide Technology, edited by D. K. Ferry, SAMS, 1985.

24. Nuss, M. C., and Auston, D. H., "Direct Subpicosecond Measurements of Carrier Mobility of Photoexcited Electrons in GaAs" in Picosecond Electronics and Optoelectronics II, edited by F. J. Leonberger, Springer-Verlag, 1987.

25. Auston, D. H., Picosecond Optoelectronic Devices, edited by Chi H. Lee, Academic Press Inc., 1984, p. 73.

26. Van Zeghbroek, J., Patrick, W., Halbout, J.-M., and Vettiger, P., IEEE Transactions on Electron Devices, Vol. 7, p. 2493, 1990.

27. Klingenstein, M., Kuhl, J., Rosenzweig, J., Moglestue, C., and Axmann, A., Applied Physics Letters, Vol. 70, p. 2435, 1991.

28. Van Exter, Martin, and Grischkowsky, Daniel, IEEE Transactions on Microwave Theory and Techniques, MTT-38, p. 1684, 1990.

29. Kingston, R. H., Detection of Optical and Infrared Radiation, Springer-Verlag, Berlin, 1978, p. 59.

30. Ho, P., Kao, M. Y., Chao, P. C., Duh, K. H. G., Ballingall, J. M., Allen, S. T., Tessmer, A. J., and Smith, P. M., Electronics Letters, Vol. 27, p. 325, 1991.

31. Frankel, M. Y., Whitaker, J. F., Mourou, G. A., and Valdmanis, J. A., "Ultrahigh-Bandwidth Vector Network Analyzer Based on External Electro-Optic Sampling." Solid-State Electronics, Vol. 35, pp. 325–332, March 1992.

32. Lee, C. H., "Picosecond Optics and Microwave Technology." IEEE Transactions on Microwave Theory and Techniques, Vol. 38, pp. 596-607, May 1990.

33. Kim, J., Williamson, S., Nees, J., Wakana, S., and Whitaker, J., "Photoconductive Sampling Probe with 2.3-ps Temporal Resolution and 4-μV Sensitivity", Applied Physics Letters, Vol. 62, No. 18, 3 May 1993 .

34. Spindt, C., Brodie, I., Humphrey, L., and Westerberg, E., "Physical Properties of Thin Film Field Emission Cathodes with Molybdenum Cones." Journal of Applied Physics, Vol. 37, No. 12, December 1976.

35. Kim, J., Williamson, S., Nees, J., and Wakana, S., A Novel Free-Standing Absolute-Voltage Probe With 2.3-Picosecond Resolution and 1-Microvolt Sensitivity, Paper presented at Ultrafast Phenomena VII, Antibes-Juan-Les-Pins, France, 8–12 June 1992.

WRITTEN PUBLICATIONS LIST

Motet, T., Nees, J., Williamson, S., and Mourou, G., "1.4 ps Rise-Time High-Voltage Photoconductive Switching." Applied Physics Letters, Vol. 59, No. 12, pp. 1455–1457, Sep. 16, 1991.

Chen, Y., Williamson, S., Brock, T., Smith, F. W., and Calawa, A. R., "375-GHz-Bandwidth Photoconductive Detector." Applied Physics Letters, Vol. 59, pp. 1984–1986, Oct. 14, 1991.

Gupta, S., Williamson, S. L., Chen, Y., Whitaker, J. F., and Smith, F. W., "Epitaxial Methods Produce Robust Ultrafast Detectors." Laser Focus World, Vol. 28, pp. 97–104, June 1992.

Chen, Yi, Williamson, Steven, and Brock, Tim, "1.9 Picosecond High-Sensitivity Sampling Optical Temporal Analyzer." Applied Physics Letters, Vol. 64, No. 5, pp.551–553, January 31, 1994.

PROFESSIONALS ASSOCIATED WITH THE RESEARCH EFFORT

John A. Nees, Steven L. Williamson, Gérard A. Mourou

Degrees Granted: Yi Chen, PhD in Electrical Engineering, University of Michigan, May 1991, *Development of Detectors and Modulators for Multi-Hundred Gigahertz Operation*

INTERACTIONS: CONFERENCE PAPERS

Nees, J., Ultrafast Detector, Temporal Analyzer, and Probe, Paper presented at Ultrafast Electronics and Optoelectronics, San Francisco, CA, January 1993.

Chen, Y., Williamson, S. L., Brock, T., and Smith, F. W., 1.9-ps Optical Temporal Analyzer Using 1.2-ps Photodetector and Gate, Paper presented at IEEE International Electron Device Meeting, Boston, MA, December 1991.

Williamson, S., Chen, Y., Craig, D., and Mourou, G., Development of a Multi-Hundred-Gigahertz Electro-Optic Modulator and Photodetector, Paper presented at DOD Fiber Optics '92, p. 271 of Proceedings, 1992.

Motet, T., Nees, J., Williamson, S., and Mourou, G., Picosecond High-Voltage Pulses Generated Using Low-Temperature GaAs, Paper presented at Conference of Research Materials Society, Boston, MA, 1991.

Chen, Y., Williamson, S. L., Brock, T., Smith, F. W., and Calawa, A. R., Multi-Hundred-Gigahertz Photodetector Development, Paper presented at Conference of Research Materials Society, Boston, MA, 1991.

Motet, T., Nees, J., Williamson, S., and Mourou, G., Picosecond Photoconductive Switching, Paper presented at Picosecond Electronics and Optoelectronics IV, Salt Lake City, UT, March 1991.

Chen, Y., Nees, J., and Williamson, S., Propagation of Picosecond Electrical Pulses in GaAs for Velocity-Matched Modulators, Paper presented at Picosecond Electronics and Optoelectronics IV, Salt Lake City, UT, March 1991.

Motet, T., Nees, J., Williamson, S., and Mourou, G., Single-Picosecond High-Voltage Photoconductive Switching Using Low-Temperature-Grown GaAs, Paper presented at Conference on Lasers and Electro-Optics, Baltimore, MD, May 1991.

Chen, Y., Williamson, S. L., and Brock, T., 1.2-ps High-Sensitivity Photodetector/Switch Based on Low-Temperature-Grown GaAs, Paper presented at Conference on Lasers and Electro-Optics, Baltimore, MD, May 1991.

PATENT APPLICATIONS

1-Picosecond High-Sensitivity Photoconductor, Steven Williamson and Yi Chen, 5 May 1992, S/N 07/882,055.

High-Speed High-Impedance External Photoconductive-Type Sampling Probe/Pulser, Steven Williamson, 12 May 1992, S/N 07/882,503.

*U.S. GOVERNMENT PRINTING OFFICE: 1996-710-126-20254

MISSION

OF

ROME LABORATORY

Mission. The mission of Rome Laboratory is to advance the science and technologies of command, control, communications and intelligence and to transition them into systems to meet customer needs. To achieve this, Rome Lab:

a. Conducts vigorous research, development and test programs in all applicable technologies;

b. Transitions technology to current and future systems to improve operational capability, readiness, and supportability;

c. Provides a full range of technical support to Air Force Materiel Command product centers and other Air Force organizations;

d. Promotes transfer of technology to the private sector;

e. Maintains leading edge technological expertise in the areas of surveillance, communications, command and control, intelligence, reliability science, electro-magnetic technology, photonics, signal processing, and computational science.

The thrust areas of technical competence include: Surveillance, Communications, Command and Control, Intelligence, Signal Processing, Computer Science and Technology, Electromagnetic Technology, Photonics and Reliability Sciences.